Lawrence Berkeley National Laboratory
Recent Work

Title
Induced seismicity in Oklahoma affects shallow groundwater

Authors
Wang, CY
Manga, M
Shirzaei, M
et al.

Peer reviewed

Induced Seismicity in Oklahoma Affects Shallow Groundwater

Chi-Yuen Wang, Michael Manga, Manoochehr Shirzaei, Matthew Weingarten, and Lee-Ping Wang

Chi-Yuen Wang and Michael Manga: Department of Earth and Planetary Science University of California Berkeley McCone Hall Berkeley, California 94720-4767 U.S.A. chiyuen@berkeley.edu; Manoochehr Shirzaei: School of Earth and Space Exploration Arizona State University Tempe, Arizona 85281 U.S.A.; Matthew Weingarten: Department of Geophysics Stanford University 397 Panama Street Stanford, California 94305 U.S.A.; Lee-Ping Wang: Department of Chemistry University of California Davis 1 Shields Avenue Davis, California 95616 U.S.A.

ABSTRACT

Documentation and analysis of groundwater responses to induced earthquakes are important to better understand their influence on shallow groundwater systems and hydrogeological properties and processes. Here we show that induced seismicity in Oklahoma can cause changes of groundwater level over distances >150 km from the epicenter. We test existing models for the cause of the observed responses and find that the model most consistent with observations is enhanced crustal permeability produced by seismic waves, changing aquifer recharge. Simulation suggests that the sources of this recharge are close to the responding wells and have lateral dimensions of ~100 m. Continuous monitoring of pressure and temperature in wells, installing clustered wells to monitor multiple water levels near injection sites, and isotopic and chemical analysis of groundwater near injection sites are required to better understand and quantify the recharging sources.

INTRODUCTION

A sharp increase of seismicity has occurred in the central United States in recent years, often near "high-rate injection sites" where billions of gallons of coproduced water from hydrocarbon extraction are injected into the subsurface for disposal or to enhance production (e.g., Frohlich, 2012; Ellsworth, 2013; Keranen $et\ al.$, 2013, 2014; Hornbach $et\ al.$, 2015; McGarr $et\ al.$, 2015; Walsh and Zoback, 2015; Weingarten $et\ al.$, 2015). Three $M_w \geq 5$ earthquakes occurred in Oklahoma alone since the beginning of 2016 (Fig. 1). A growing body of evidence suggests that induced seismicity and surface deformation are coupled in complex and unexpected ways (Shirzaei $et\ al.$, 2016). A great concern is whether injection and hydrofracturing processes may impact shallow groundwater systems (e.g., Vidic $et\ al.$, 2013; Stokstad, 2014; Vengosh $et\ al.$, 2014). Natural earthquakes are known to cause a wide spectrum of hydrologic responses (e.g., Wang and Manga, 2010); thus, it is not surprising that earthquakes induced by wastewater injection may also cause similar changes. Documentation and analysis of groundwater responses to induced earthquakes, however, are important to better understand how induced seismicity may affect hydrogeological processes and shallow groundwater systems in the United States and elsewhere. After the 2016 M_w 5.8 Pawnee earthquake, an increase in stream discharge occurred near the epicenter of the earthquake (Manga $et\ al.$, 2016). It was

shown that earthquake-enhanced recharge may have provided the increased discharge, but the source of the excess water was not identified.

Here, we report changes of groundwater level over distances >150 km from the epicenter following the 2016 M_w ≥5.0 earthquakes in Oklahoma (Fig. 1). We discuss the mechanism of the changes by testing the existing hypotheses against observations and show that the observed changes are most consistent with the model of enhanced permeability produced by seismic waves. We simulate the observed changes and show that the changes of groundwater level were due to coseismic recharge from pre-existing sources near the wells. Finally, we highlight some important but unanswered issues.

OBSERVATION

Two types of aquifers are found in Oklahoma, in the Quaternary alluvial and terrace deposits and in the Paleozoic bedrock, with the former being the most important supplier for agricultural, municipal, and domestic use. The alluvial and terrace deposits consist of subhorizontal lenticular beds of sand, silt, clay, and gravel, which vary greatly in thickness within short lateral distances (Wood and Burton, 1968). All wells used in this study are open to aquifers in this formation.

The U.S. Geological Survey (USGS) manages 39 wells in Oklahoma; these were installed for monitoring groundwater level and equipped with automated recording equipment that continuously takes data at fixed intervals of 15–60 min. Data are transmitted to the USGS every hour. Most USGS wells are located away from the injection sites (Fig. 1); only two wells (364821 and 364831, Fig. 1 and Table 1) are located among many, and within 5 km from some injection wells. The Oklahoma Water Resource Board (OWRB) manages numerous groundwater wells for irrigation, municipal, and domestic use. The vast majority of measurements are manually collected, but some OWRB wells have pressure transducers that provide hourly measurements of water level.

The three 2016 M_w ≥5.0 earthquakes in Oklahoma all have strike-slip mechanisms (Fig. 1) and relatively shallow focal depths (Table 1). Aftershocks are not plotted in Figure 1 in order not to clutter the figure. The 13 February M_w 5.1 earthquake near Fairview ruptured a 70° dipping, southwest–northeast (SW–NE)-trending buried fault (Yeck *et al.*, 2016); the 3 September M_w 5.8 earthquake near Pawnee probably ruptured a previously unmapped northwest–southeast (NW–SE)-trending fault (Bennett *et al.*, 2016); and the 6 November M_w 5.0 earthquake near Cushing probably ruptured an SW–NE-trending fault (USGS, 2016).

Two USGS wells (364821 and 364831, Fig. 1), located 159 and 156 km from the epicenter, respectively, responded to the 6 November M_w 5.0 earthquake near Cushing. Water levels in the wells started to rise immediately after the earthquake (Fig. 2a,b) and continued to rise for 10–20 hrs before reaching

their respective maxima of 4–7 cm above the pre-earthquake levels; afterward water levels slowly declined. Barometric pressure was stable at the time of the earthquake (see Fig. S1, available in the electronic supplement to this article), and no notable precipitation occurred several days before or after this earthquake. Furthermore, no similar change occurred in the records at other times. Thus, these water-level changes are likely to be directly related to the M_w 5.0 earthquake. Two OWRB wells (18699 and 171706, Fig. 1) responded to the 13 February M_w 5.1 Fairview earthquake. Well 18699 is 2.6 km from the epicenter and documented a coseismic rise of water level that continued to rise for several hours to reach a maximum of ~10 cm above the pre-earthquake level (Fig. 2c). Well 171706 is 81 km from the epicenter and showed a coseismic decrease of water level with continued decrease until being interrupted by a rapid rise of water level a day later (Fig. 2d). No rainfall occurred in the period several days before or after this earthquake. During the 3 September M_w 5.8 Pawnee earthquake, a change of water level was documented in OWRB well 127105 (Fig. 2e). Substantial rainfalls occurred both before and after this earthquake but none at the time of the earthquake. Rainfall leads to immediate rise of water level in the wells, suggesting surface runoff entering the well; the water-level rise after each rainfall was followed by a rapid water-level decline. The coseismic change of water level was followed by a sharp reversal in water level a few days later. A similar effect of rainfall may also have influenced water level in well 364821 during this time interval (top right panel), but no daily precipitation data are available near this well.

Despite the differences in polarities and epicenter distances, all responses discussed above share one common characteristic: water level following the coseismic change continued to change in the same direction for several hours to several days to reach maxima or minima before it gradually declined. This is similar to the water-level response of the Bourdieu Valley well near Parkfield, California, to natural earthquakes (Roeloffs, 1998).

DISCUSSION

Several mechanisms have been proposed to explain water-level changes during earthquakes; these include static strain due to fault rupture (Wakita, 1975; Muir-Wood and King, 1993; Ge and Stover, 2000; Chia *et al.*, 2008), coseismic liquefaction (Roeloffs, 1998; Manga, 2001), and earthquake-enhanced permeability by dynamic stresses (Rojstaczer *et al.*, 1995; Fleeger and Goode, 1999; Brodsky *et al.*, 2003). The location of the earthquakes (Fig. 1) shows that all wells are located in areas of postseismic static extension, inconsistent with the observed increases of water level at the two USGS wells (364821 and 364831) and the OWRB well 18669. Furthermore, the calculated static volumetric strain (Okada, 1992; see Table S1) at the OWRB well 171706 due to the 13 February M_w 5.1 earthquake is too small to explain the coseismic decrease of water level (Fig. 2d). For these reasons, we do not favor the static strain hypothesis for the observed coseismic change of water level.

The occurrence of liquefaction after the 3 September M_w 5.8 earthquake (Kolawole *et al.*, 2016; Manga *et al.*, 2016) adds weight to the model of liquefaction by dynamic strain. We test this hypothesis for the present case with the magnitude of the dynamic strain that may be estimated from the peak ground velocity (PGV) in the vicinity of the wells (see Data and Resources). Seismographic records from several stations near the wells show PGV of 0.2–0.3 cm/s. Assuming a shear velocity of 500 m/s for wet sands and gravels (Press, 1966), the peak dynamic shear strain is ~5×10^{-6}, much smaller than the threshold amplitude of cyclic shear strains (10^{-4}) required to initiate undrained consolidation in saturated sands, according to experiments on various kinds of sands under different confined environments (Vucetic, 1994). Furthermore, the occurrence of earthquake-induced liquefaction is delimited by a threshold of seismic energy density of ~0.1 J/m^3 ; that is, the liquefaction limit that is shown as a straight line on a plot of hypocentral distance versus earthquake magnitude (Wang, 2007; Fig. 3). Plotting the responding wells on this diagram shows that most wells fall beyond the liquefaction limit (Fig. 3) at distances where the seismic energy density is below that required for liquefaction. For these reasons, we also do not favor the liquefaction model.

We next test the model of enhanced permeability by dynamic stresses. We consider a one-dimensional aquifer of length L (Fig. 4a); recharge is assumed to occur at the time of the earthquake along a section of the aquifer (between L_1 and L_2). The differential equation for the coseismic change of hydraulic head h in a confined aquifer and the linearized Boussinesq equation for an unconfined aquifer have the same form:

$$\frac{\partial h}{\partial t} = D\frac{\partial^2 h}{\partial x^2} + w(x, t), \tag{1}$$

in which D is the hydraulic diffusivity and $w(x,t)$ is the coseismic change of water level per unit time due to recharge. In the present context, we use equation (1) as the linearized Boussinesq equation for an unconfined aquifer. Thus, $D=T/S_y$, in which T is the transmissivity and S_y is the specific yield of the aquifer; these parameters may be evaluated from well tests.

For boundary conditions, we consider no flow on one end of the aquifer to represent the presence of faults that block groundwater flow and zero head on the other end to represent discharge to local creeks. Thus,

$$\frac{\partial h}{\partial x} = 0 \quad \text{at} \quad x = 0, \quad \text{and} \quad h = 0 \quad \text{at} \quad x = L. \tag{2}$$

We further assume that, during the earthquake, w is finite for a short time, with the cumulative change being W_o between L_1 and L_2 along the aquifer but zero elsewhere. The solution for h is (see the electronic supplement)

$$b(x,t)=\frac{4W_o}{\pi}\sum_{n=1}^{\infty}\frac{1}{n}\cos\left(\frac{n\pi x}{2L}\right)e^{-\frac{n^2\pi^2 D_t}{4L^2}}\left[\sin\frac{n\pi L_2}{2L}-\sin\frac{n\pi L_1}{2L}\right].$$

(3)

We limit the simulation to the responses of the two USGS wells (Fig. 2a,b); the records in the OWRB wells were either too noisy to simulate (Fig. 2c) or were interrupted by additional changes (Fig. 2d). The nonlinear least-square method is used to fit equation (3) to the increased water level after the earthquake. Equation (3) has five independent parameters x/L, L_1/L, L_2/L, W_o, and D/L^2. We tried different values of D/L^2 while keeping the rest as free parameters. The model with $D/L^2=3\times10^{-7}$ s^{-1} yields the smallest root mean square residuals and is chosen as the best model. Table 2 lists the best-fitting parameters and their uncertainties. Figure 4b,c shows the best-fitting curves together with the data for increased water levels.

Well tests and hydrogeological simulation of groundwater flow in the alluvial and terrace aquifer (Havens, 1989) yield $T=0.0075$ m^2/s and $S_y=0.15$, which give $D=0.05$ m^2/s . Using this D together with $D/L^2=3\times10^{-7}$ s^{-1}, we obtain $L\sim400$ m. This value of L is qualitatively consistent with geologic observations that the alluvial and terrace deposits consist mostly of lenticular beds of sand, silt, clay, and gravel, which vary greatly in thickness over short lateral distances (Wood and Burton, 1968). The simulation also suggests that the water-level increases in the two wells were caused by independent sources with widths of ~100 m (L_2–L_1) and ~20 m from the respective wells (L_1–x).

An important question is why some USGS wells closer to the 6 November M_w 5.0 earthquake than the responding wells (Fig. 1) did not show a coseismic response. Different lithologies may not explain the different responses because many nonresponding wells are installed in similar alluvial sediments as the responding wells in this study. Another possible reason is that the responding USGS wells are closer to a large number of injection wells than the nonresponding wells (Fig. 1), but the nature of the recharging source remains unclear. It is also difficult to explain why the two USGS wells that responded to the 6 November M_w 5.0 earthquake did not respond to the much closer 13 February M_w 5.1 earthquake or the much larger 3 September M_w 5.8 earthquake. We speculate that the first two earthquakes may have primed the aquifer, bringing it closer to the threshold for permeability change, and that the last earthquake, although smaller and further away, was the last increment that pushed the aquifer over the threshold to increase permeability. In addition, several studies have shown that earthquake triggering of seismicity and water-level changes depend on the frequency of seismic waves (e.g., Brodsky and Prejean, 2005; Wong and Wang, 2007; Guilhem et al., 2010; Rudolph and Manga, 2012). Thus, the answer to the question about why wells only sometimes respond to

earthquakes may require a thorough analysis of the spectral content of seismic waves recorded at stations near the wells following each earthquake.

Finally, as noted earlier, the coseismic decrease of water level in well 171707 was followed a day later by a sharp increase of water level, and the coseismic increase of water level in well 127105 was followed a few days later by a sharp decrease of water level. It is noteworthy that the reversal after the 3 September M_w 5.8 Pawnee earthquake was preceded immediately by an M_w 2.7 aftershock near the well, and the reversal after the 13 February M_w 5.1 Fairview earthquake was preceded by three aftershocks of M_w >3.5 near the well on the same day. Although we cannot rule out the possibility that the coincidences in time between the reversals of water-level changes and aftershocks were accidental, laboratory study of permeability of fractured rocks (e.g., Liu and Manga, 2009) shows that cyclic loading can either increase or decrease permeability; thus, it is not unlikely that aftershocks can reverse the permeability changes induced by the mainshock, causing a reversal in the coseismic change of water level.

CONCLUDING REMARKS

In this study, we document coseismic changes of groundwater level in Oklahoma after three induced earthquakes with magnitude greater or equal to 5.0. We showed that the observed changes can be explained neither by the static strain hypothesis nor by the liquefaction hypothesis. On the other hand, the model of enhanced crustal permeability produced by seismic waves, altering recharge of shallow aquifers, is consistent with observations. Simulations based on this model suggest that the sources of this recharge are close to the responding wells and have lateral dimensions of ~100 m. Further testing of this model and better understanding and quantifying the influence of induced earthquakes on shallow groundwater systems require continuous monitoring of pressure and temperature in wells, installing clustered wells to monitor multiple water levels near injection sites, tidal analysis of water level in wells, and isotopic and chemical analysis of groundwater near injection sites.

DATA AND RESOURCES

The U.S. Geological Survey (USGS) water-level data are available from http://waterdata.usgs.gov/ (last accessed January 2017), and the Oklahoma Water Resource Board (OWRB) water-level data are available from http://www.owrb.ok.gov/ (last accessed January 2017). The peak ground velocity (PGV) in the vicinity of wells is available at http://earthquake.usgs.gov/earthquakes/eventpage/us100075y8#map? ShakeMap (last accessed January 2017) Stations=true&shakemapSource=us&shakemapCode=us100075y8.

REFERENCES

Bennett, S. E. K., A. R. Streig, J. C. Chang, K. T. Hornsby, I. E. Woelfel, R. D. Andrews, R. W. Briggs, D. E. McNamara, R. A. Williams, and D. J. Wald (2016). Rapid response to the 3 September 2016 M 5.8 earthquake near Pawnee, Oklahoma: Summary of structural damage and liquefaction observations, AGU Fall Meeting, Abstract S44C–01.

Brodsky, E. E., and S. G. Prejean (2005). New constraints on mechanisms of remotely triggered seismicity at Long Valley Caldera, J. Geophys. Res. 110, doi: 10.1029/2004JB003211.

Brodsky, E. E., E. Roeloffs, D. Woodcock, I. Gall, and M. Manga (2003). A mechanism for sustained groundwater pressure changes induced by distant earthquakes, J. Geophys. Res. 108, doi: 10.1029/ 2002JB002321.

Chia, Y., J. J. Chiu, Y. H. Jiang, T. P. Lee, Y. M. Wu, and M. J. Horng (2008). Implications of coseismic groundwater level changes observed at multiple-well monitoring stations, Geophys. J. Int. 172, 293–301.

Ellsworth, W. L. (2013). Injection-induced earthquakes, Science 341, 1,225,942–1,225,943. Fleeger, G. M., and D. J. Goode (1999). Hydrologic effects of the Pymatuning earthquake of September 25, 1999, in northwestern Pennsylvania, U.S. Geol. Surv. Water-Res. Investig. Rept. 99-4170.

Frohlich, C. (2012). Two-year survey comparing earthquake activity and injection-well locations in the Barnett Shale, Texas, Proc. Natl. Acad. Sci. Unit. States Am. 109, 13,934–13,938.

Ge, S., and C. Stover (2000). Hydrodynamic response to strike- and dipslip faulting in a half space, J. Geophys. Res. 105, 25,513–25,524.

Guilhem, A., Z. Peng, and R. M. Nadeau (2010). High-frequency identification of non-volcanic tremor triggered by regional earthquakes, Geophys. Res. Lett. 37, no. 16, doi: 10.1029/2010GL044660.

Havens, J. S. (1989). Geohydrology of the alluvial and terrace deposits of the North Canadian River from Oklahoma City to Eufaula Lake, central Oklahoma, U.S. Geol. Surv. Water-Res. Investig. Rept. 88- 4234.

Hornbach, M. J., H. R. DeShon, W. L. Ellsworth, B. W. Stump, C. Hayward, C. Frohlich, H. R. Oldham, J. E. Olson, M. B. Magnani, C. Brokaw, and J. H.

Luetgert (2015). Causal factors for seismicity near Azle, Texas, Nature Comm. 6, doi: 10.1038/ncomms7728.

Keranen, K. M., H. M. Savage, G. A. Abers, and E. S. Cochran (2013). Potentially induced earthquakes in Oklahoma, USA: Links between wastewater injection and the 2011 Mw 5.7 earthquake sequence, Geology 41, no. 6, doi: 10.1130/G34045.1.

Keranen, K. M., M. Weingarten, G. A. Abers, B. A. Bekins, and S. Ge (2014). Sharp increase in central Oklahoma seismicity since 2008 induced by massive wastewater injection, Science 345, 448–451, doi: 10.1126/science.1255802.

Kolawole, F., A. M. Ismail, C. M. Pickens, D. Beckendorff, M. V. Mayle, J. F. Goussi, V. Nyalugwe, A. Aghayan, S. Tim, and E. A. Atekwana (2016). Geophysical investigation of liquefaction and surface rup tures at selected sites in Oklahoma post the 2016 Mw 5.8 Pawnee, OK earthquake, AGU Fall Meeting, Abstract S51E–3164.

Liu, W., and M. Manga (2009). Changes in permeability caused by dynamic stresses in fractured sandstone, Geophys. Res. Lett. 36, L20307, doi: 10.1029/2009GL039852.

Manga, M. (2001). Origin of postseismic streamflow changes inferred from baseflow recession and magnitude-distance relations, Geophys. Res. Lett. 28, 2133–2136.

Manga, M., C.-Y. Wang, and M. Shirzaei (2016). Increased stream discharge after the 3 September 2016 Mw 5.8 Pawnee, Oklahoma earthquake, Geophys. Res. Lett. 43, no. 22, doi: 10.1002/2016GL071268.

McGarr, A., B. Bekins, N. Burkardt, J. Dewey, P. Earle, W. Ellsworth, S. Ge, S. Hickman, A. Holland, E. Majer, et al. (2015). Coping with earthquakes induced by fluid injection, Science 347, 830–831, doi: 10.1126/science.aaa0494.

Muir-Wood, R., and G. C. P. King (1993). Hydrological signatures of earthquake strain, J. Geophys. Res. 98, 22,035–22,068.

Okada, Y. (1992). Internal deformation due to shear and tensile faults in a half space, Bull. Seismol. Soc. Am. 82, 1018–1040.

Press, F. (1966). Seismic velocities, in Handbook of Physical Constants, S. P. Clark Jr. (Editor), Geol. Soc. Am., Memoir, Vol. 97, New York, New York, 195–218.

Roeloffs, E. A. (1998). Persistent water level changes in a well near Parkfield, California, due to local and distant earthquakes, J. Geophys. Res. 103, 869–889.

Rojstaczer, S., S. Wolf, and R. Michel (1995). Permeability enhancement in the shallow crust as a cause of earthquake-induced hydrological changes, Nature 373, 237–239.

Rudolph, M. L., and M. Manga (2012). Frequency dependence of mud volcano response to earthquakes, Geophys. Res. Lett. 39, doi: 10.1029/2012GL052383.

Shirzaei, M., W. L. Ellsworth, K. Tiampo, P. J. Gonzalez, and M. Manga (2016). Surface uplift and time-dependent seismic hazard due to fluid injection in eastern Texas, Science 353, 1416–1419, doi: 10.1126/science.aag0262.

Stokstad, E. (2014). Will fracking put too much fizz in your water? Science 344, 1468.

U.S. Geological Survey (USGS) (2016). M 5.0 North Central Oklahoma Earthquake of 07 November 2016, available at …https://earthquake .usgs.gov/earthquakes/eqarchives/…/20161107.pdf (last accessed January 2017).

Vengosh, A., R. B. Jackson, N. Warner, T. Darrah, and A. Kondash (2014). A critical review of the risks to water resources from unconventional shale gas development and hydraulic fracturing in the United States, Environ. Sci. Technol. 48, 8334–8348.

Vidic, R. D., S. L. Brantley, J. M. Vandenbossche, D. Yoxtheimer, and J. D. Abad (2013). Impact of shale gas development on regional water quality, Science 340, doi: 10.1126/science.1235009.

Vucetic, M. (1994). Cyclic threshold shear strains in soils, J. Geotech. Eng. 120, 2208–2228.

Wakita, H. (1975). Water wells as possible indicators of tectonic strain, Science 189, 553–555.

Walsh, F. R., and M. D. Zoback (2015). Oklahoma's recent earthquakes and saltwater disposal, Sci. Adv. doi: 10.1126/sciadv.1500195.

Wang, C.-Y. (2007). Liquefaction beyond the near field, Seismol. Res. Lett. 78, 512–517.

Wang, C.-Y., and M. Manga (2010). Earthquakes and water, in Lecture Notes in Earth Science, J. Reitner, M. H. Trauth, K. Stuwe, and D. Yuan (Editors), Vol. 114, Springer, Berlin, Germany, 249 pp.

Weingarten, M., and S. Ge (2014). Insights into water level response to seismic waves: A 24 year high-fidelity record of global seismicity at Devils Hole, Geophys. Res. Lett. 41, doi: 10.1002/2013GL058418.

Weingarten, M., S. Ge, J. W. Godt, B. A. Bekins, and J. L. Rubinstein (2015). High-rate injection is associated with the increase in U.S. mid-continent seismicity, Science 348, 1336–1340.

Wong, A., and C.-Y. Wang (2007). Field relations between the spectral composition of ground motion and hydrological effects during the 1999 Chi-Chi (Taiwan) earthquake, J. Geophys. Res. 112, no. B10305, doi: 10.1029/2006JB004516.

Wood, P. R., and L. C. Burton (1968). Groundwater resources of Cleveland and Oklahoma Counties, Oklahoma, Oklahoma Geol. Surv. Circular 71, 75 pp.

Yeck, W. L., M. Weingarten, H. M. Benz, D. E. McNamara, E. A. Bergmann, R. B. Herrmann, J. L. Rubinstein, and P. S. Earle (2016). Farfield pressurization likely caused one of the largest injection induced earthquakes by reactivating a large preexisting basement fault structure, Geophys. Res. Lett. 43, no. 19, 10,198–10,207, doi: 10.1002/ 2016GL070861.
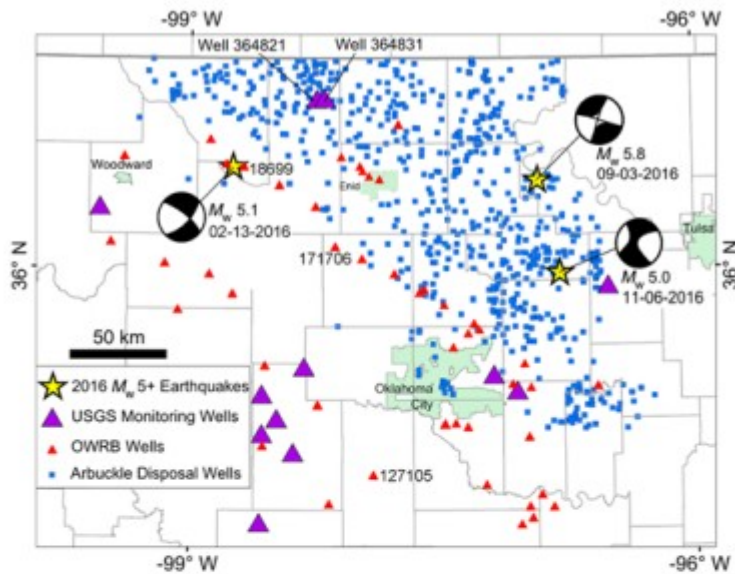
▲ **Figure 1.** Locations of the epicenters (yellow stars) and focal mechanism of three 2016 $M_w \geq 5$ earthquakes in Oklahoma; smaller earthquakes are not plotted in order not to clutter the diagram. The locations of U.S. Geological Survey (USGS) wells (large triangles) and Oklahoma Water Resource Board (OWRB) wells (small triangles) are also plotted. The responding wells are labeled with identification numbers. Injection wells operating in the Arbuckle formation, which dispose waste fluid from oil and gas production, are shown with squares. The color version of this figure is available only in the electronic edition.

| Table 1				
Earthquakes and Wells in This Study				
Name of Earthquake	**Time (UTC)** **(yyyy/mm/dd hh:mm:ss)**	**_M_w**	**Epicenter** **Location (°)**	**Depth (km)**
Fairview	2016/02/13 17:07:05	5.1	36.490, −98.709	8.3
Pawnee	2016/09/03 12:02:44	5.8	36.431, −96.931	5.6
Cushing	2016/11/07 01:44:24	5.0	35.984, −96.798	5.0
Name of Well	**Location (°)**	**Elevation (m)**	**Screen** **Depth (m)**	**Lithology**	**Epicenter Distance (km)**
USGS 364821	36.806, −98.247	348	0–8.8	Alluvial	Fairview: 54 Pawnee: 125 Cushing: 159
USGS 364831	36.809, −98.201	346	0–6.9	Alluvial	Fairview: 58 Pawnee: 121 Cushing: 156
OWRB 18699	36.496, −98.681	458	15–21	Alluvial	Fairview: 2.6 Pawnee: 157 Cushing: 178
OWRB 171706	36.056, −97.981	347	0–16	Alluvial	Fairview: 81 Pawnee: 103 Cushing: 107
OWRB 127105	35.032, −97.915	328	22–27 30–33	Alluvial Shale	Fairview: 177 Pawnee: 179 Cushing: 146

USGS, U.S. Geological Survey; OWRB, Oklahoma Water Resource Board.
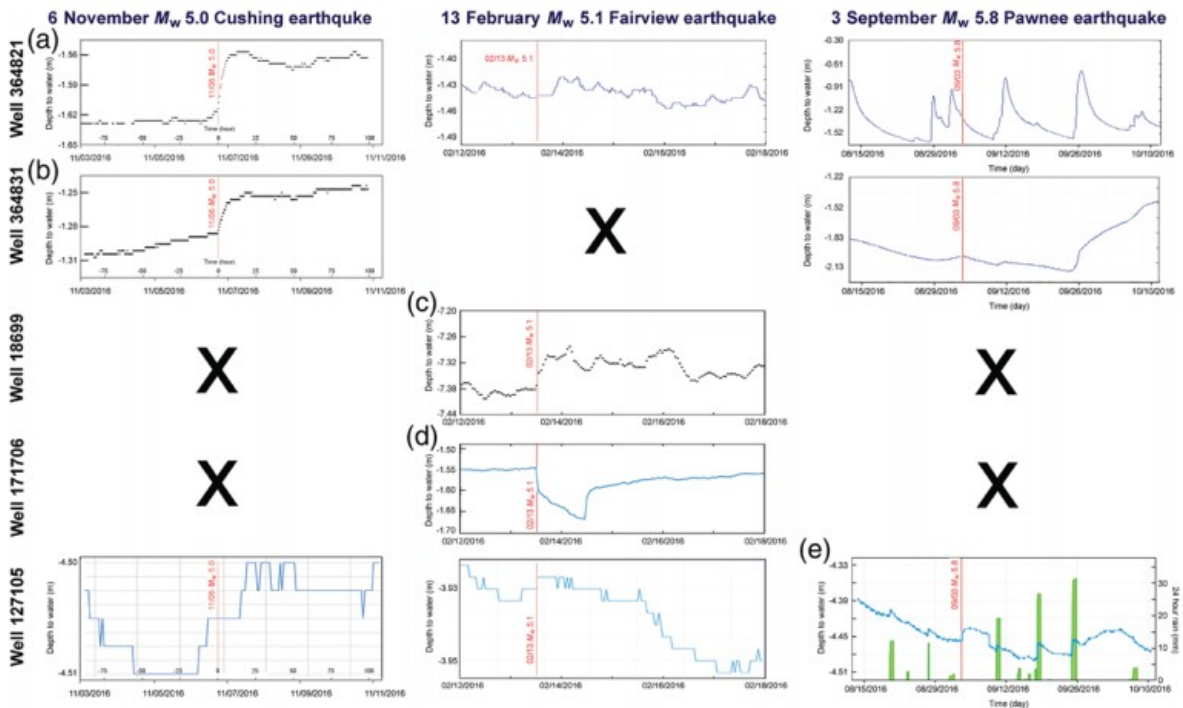
▲ **Figure 2.** Water level in five wells before and after the three M_w >5.0 earthquakes in Oklahoma in 2016. Bold X indicates cases with no data; vertical lines show the time of the earthquakes. For clarity, only panels with coseismic changes of water level that are also discussed are labeled. (a) Coseismic change of water level in USGS well 364821 during the 6 November M_w 5.0 Cushing earthquake. (b) Coseismic change of water level in USGS well 364831 during the 6 November M_w 5.0 Cushing earthquake. (c) Coseismic change of water level in OWRB well 18699 before and after the 13 February M_w 5.1 earthquake. (d) Coseismic change of water level in OWRB well 171706 before and after the 13 February M_w 5.1 earthquake. (e) Coseismic change of water level in OWRB well 127105 (blue curve) before and after the 3 September M_w 5.8 Pawnee earthquake. Daily precipitation is shown in vertical bars. The color version of this figure is available only in the electronic edition.
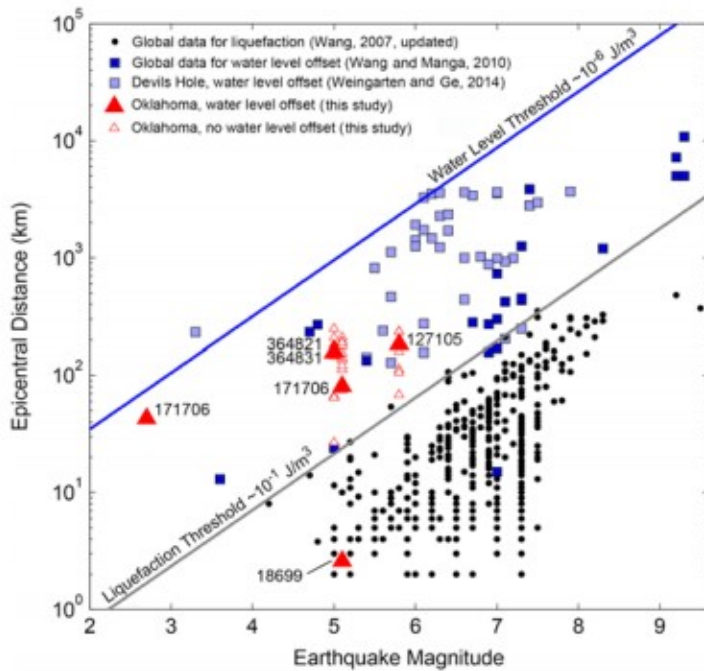
▲ **Figure 3.** Occurrences of earthquake-induced water-level changes and liquefaction plotted on a diagram of hypocentral distance versus earthquake magnitude. Straight lines show contours of equal seismic energy density; the uppermost line corresponds to a seismic energy density of 10^{-6} J/m^3, the threshold energy density required to trigger water-level change; the lower line marks the threshold energy density of 30 J/m^3 required to trigger liquefaction in sensitive soils (Wang, 2007). Responding wells of this study (filled triangles) are labeled with identification numbers; wells 364821 and 364831 overlap on this diagram. Nonresponding USGS wells are plotted as open triangles; nonresponding OWRB wells are not plotted because many wells do not have data of the required quality to be characterized. Data for global water-level changes are taken from a compilation (Wang and Manga, 2010; dark squares) and a recent study at Devils Hole (Weingarten and Ge, 2014; light squares). Liquefaction occurrences (black dots) are taken from a global compilation (Wang, 2007), with updates from New Zealand (S. Cox, personal comm., 2015). Responding wells of this study (filled triangles) are labeled with identification numbers; wells 364821 and 364831 overlap on this diagram. The plot shows that the seismic energy density at wells 364821 and 364831 during the 6 November M_w 5.0 earthquake and those at well 171706 during the 13 February M_w 5.1 earthquake are all less than the threshold energy required to trigger liquefaction but greater than that required to trigger water-level change. It also shows that the seismic energy density at well 171706 during an M_w 2.7 aftershock was greater than the threshold energy required to trigger water-level change. The color version of this figure is available only in the electronic edition.
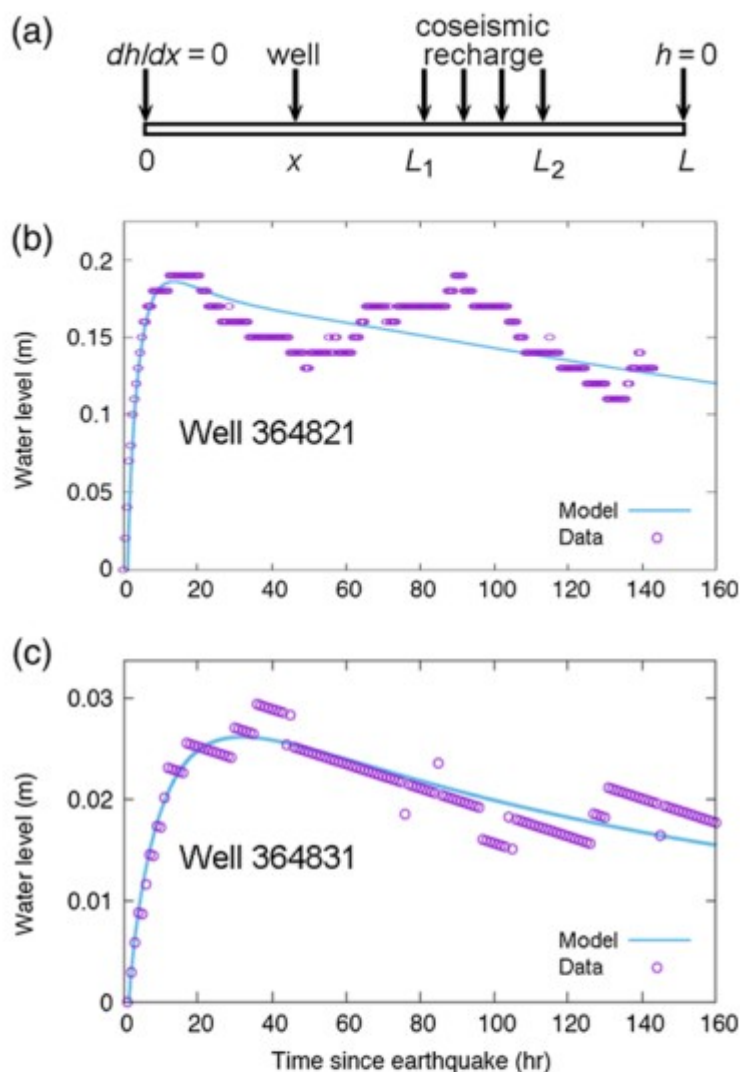
▲ **Figure 4.** (a) Schematic of model geometry and boundary conditions assumed in the simulations. (b) Observed (circles) and simulated (curve) increases of water level in well 364821 following the 2016 M_w 5.0 earthquake near Cushing, Oklahoma. Time of the earthquake is $t = 0$. Oscillations in water level about the model fit are due to oscillations in barometric pressure (Ⓔ Fig. S1, available in the electronic supplement to this article). The root mean square (rms) residual of this fit to the data is 0.020 m (Table 2). (c) Observed and simulated increases of water level in well 364831. The trend of water-level increase in this well before the earthquake (Fig. 2d) was removed from the data. The rms residual of this fit to the data is 0.002 m (Table 2). The color version of this figure is available only in the electronic edition.

Table 2
Best-Fitting Parameters and Estimated Uncertainties for Increased Water Levels in Two USGS Wells after the 6 November M_w 5.0 Cushing, Oklahoma, Earthquake

	USGS Well 36482109	USGS Well 36483109
Best-fitting parameters in equation (3)		
L_1/L	0.256 ± 0.056	0.114 ± 0.227
L_2/L	0.476 ± 0.035	0.446 ± 0.079
x/L	0.202 ± 0.018	0.067 ± 0.064
H_o (m)	0.434 ± 0.015	0.032 ± 0.014
rms residuals (m)	0.0197	0.0024
Derived parameters with $L = 400$ m (see the Discussion section)		
L_1 (m, left boundary of coseismic recharge in Fig. 4a)	102 ± 22	46 ± 91
L_2 (m, right boundary of coseismic recharge in Fig. 4a)	190 ± 14	178 ± 32
x (m, well location in Fig. 4a)	81 ± 7	27 ± 26

rms, root mean square.